A R C H I V E S O F M E T A L L U R G Y A N D M A T E R I A L S
Volume 60 2015 Issue 3
DOI: 10.1515/amm-2015-0305

M. GWOŹDZIK*,#

CHARACTERIZATION OF OXIDE LAYERS FORMED ON 13CrMo4-5 STEEL OPERATED FOR A LONG TIME AT AN ELEVATED TEMPERATURE

CHARAKTERYSTYKA WARSTW TLENKOWYCH POWSTAŁYCH NA STALI 13CrMo4-5 PODCZAS DŁUGOTRWAŁEJ EKSPLOATACJI W PODWYŻSZONEJ TEMPERATURZE

The paper contains results of studies into the formation of oxide layers on 13CrMo4-5 (15HM) steel long-term operated at an elevated temperature. The oxide layer was studied on a surface and a cross-section at the inner and outer surface of the tube wall. The 13CrMo4-5 steel operated at the temperature of 470°C during 190,000 hours was investigated. X-ray structural examinations (XRD) were carried out, microscope observation s using an optical, scanning microscope were performed. The native material chemical composition was analysed by means of emission spark spectroscopy, while that of oxide layers on a scanning microscope (EDS). The studies on the topography of the oxide layers comprised studies on the roughness plane, which were carried out using a AFM microscope designed for 2D and 3D studies on the surface. Mechanical properties of the oxide layer – steel (substrate) were characterised on the basis of scratch test. The adhesion of oxide layers, friction force, friction coefficient, scratching depth were determined as well as the force at which the layer was delaminated.

Keywords: 13CrMo4-5 steel, oxide layers, LM, XRD, SEM, AFM, scratch test

Praca zawiera wyniki badań warstw tlenkowych powstałych na stali 13CrMo4-5 (15HM) długotrwale eksploatowanej w podwyższonej temperaturze. Badania przeprowadzono na powierzchni oraz na przekroju przy powierzchni wewnętrznej i zewnętrznej ścianki rury. Badana stal 13CrMo4-5 była eksploatowana w temperaturze 470oC w czasie 190000 godzin. Na badanym materiale przeprowadzono badania XRD, obserwacje mikroskopowe przy użyciu mikroskopu optycznego i skaningowego. Skład chemiczny stali badano na emisyjnym spektrometrze iskrowym natomiast poszczególnych warstw tlenkowych przy użyciu mikroskopu skaningowego za pomocą EDS. W ramach badań topografii warstw tlenkowych przeprowadzono badania chropowatości powierzchniowej, które realizowano przy zastosowaniu mikroskopu sił atomowych AFM przeznaczonego do badań 2D i 3D. Przeprowadzono charakterystykę mechanicznych właściwości warstwa tlenków – stal (podłoże) na podstawie badań za pomocą scratch testu. Określono przyczepność warstw tlenkowych, siłę tarcia, współczynnik tarcia, głębokość zarysowania oraz siłę, przy której warstwa uległa delaminacji.

.

1. Introduction

The 13CrMo4-5 (15HM) steel is a chromium-molybdenum steel (Table 1) for operation at elevated temperatures (up to 550°C). It is used in the power industry for superheater and line pipes, plates for boiler drums and pressurised vessels, bottoms, forgings and bars for boiler parts, pressurised vessels and turbines [1].

TABLE 1
Chemical composition of 13CrMo4-5 steel acc. PN-EN 10028-2 [2], wt %

Chemical composition, wt %						
C	**Si**	**Mn**	**P**	**S**	**Cr**	Mo
0.08-0.18	Max. 0.35	0.40-1.00	0.025	0.010	0.70-1.15	0.40-0.60

The oxidation of the steels is a research topic of many resort in the world [3-15]. The stability of protective oxide layers formed on steels operating long-term at elevated temperatures is affected by: the temperature of component operation, the composition of the circulating medium and the steel composition [3, 4]. The steel, after exceeding the permissible operation temperature, lost protective properties of the oxides layer, which results in its corrosion. Also corrosion depends on the composition of the flue gas, which is related to the fuel type. Low-emission combustion techniques as well as co-firing of biomass make that aggressive components originate in the flue gas, such as: chlorides, sulphides and sulphates (K, Na), which corrosion action leads to serious corrosion damages of the aforementioned components [4].

In most cases the growth of oxides/deposits layer is accompanied by formation of pores and fissures. These defects are the dominating factor causing spalling and scaling of the

* CZESTOCHOWA UNIVERSITY OF TECHNOLOGY, 19 ARMII KRAJOWEJ AV., 42-200 CZESTOCHOWA, POLAND
# Corresponding author: gwozdzik@wip.pcz.pl

protective oxides layer. From this point of view it is important to reduce the quantity and size of pores and fissures in oxides. The literature laboratory data [5] shows that this defect of oxide structure changes with the time of exposure and it is difficult to predict.

2. Material and experimental methods

The material studied comprised specimens of 13CrMo4-5 (15HM) steel taken from a pipeline operated at the temperature of 470°C during 190,000 hours. The oxide layer was studied on a surface and a cross-section at the inner and outer surface of the tube wall.

The analysis of steel chemical composition was carried out using spark emission spectroscopy on a Spectro spectrometer (Table 2).

TABLE 2

Chemical composition of examined steel, wt %

Chemical composition, wt %						
C	**Si**	**Mn**	**P**	**S**	**Cr**	Mo
0.15	0.24	0.50	0.022	0.009	0.94	0.51

Thorough examinations of the oxide layer carried out on the inner and outer surface of tube wall comprised:

- microscopic examinations of the oxide layer were performed using an Olympus SZ61 and GX41 optical microscope,
- thickness measurements of formed oxide layers,
- chemical composition analysis of deposits/oxides using a Jeol JSM-6610LV scanning electron microscope (SEM) working with an Oxford EDS (Energy Dispersive Spectroscopy),
- X-ray (XRD) measurements; the layer was subject to measurements using a Seifert 3003T/T X-ray diffractometer and the radiation originating from a tube with a cobalt anode (λ_{Co}=0.17902 nm). XRD measurements were performed in the 20÷90° range of angles with an angular step of 0.1° and the exposure time of 4 s. To interpret the results of the diffractograms were described by a Pseudo Voight curve using the Analyze software. A computer software and DHN PBS and DHF4 + 2009 crystallographic database were used for the phase identification.
- the oxide layer surfaces were studied using an Vecco atomic force microscope,
- studies on formed oxides adhesion,
- microscopic assessment of formed scratches.

The oxide layer adhesion tests were carried out on an automated Revetest XPress Plus instrument using a diamond Rockwell indenter. The test was carried out using the following parameters: preset load of 1÷200 N, scratch 5 mm long.

Apart from the oxide layer adhesion determination the scratch test allowed also microscopic observations and the analysis of scratch line on the entire length of the pre-set force.

3. Results of examinations

The steel microstructure consists of a ferrite and bainite (Fig. 1). The structure of the studied steel is degraded to a significant extent. In places, carbide precipitates create "chains" on the boundaries. Also single creep micropores occur, situated mainly on the boundary of three grains.

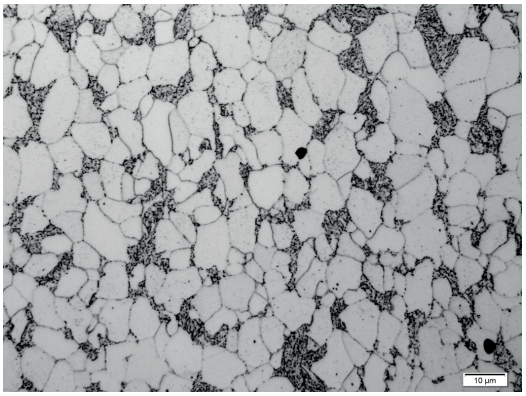

Fig. 1. Microstructure of 13CrMo4-5 steel operated for 190,000 hours at the temperature of 470°C, LM

Macroscopic observations (Fig. 2) linked with the surface topography studies carried out using the atomic forces microscopy (Fig. 3, 4) have shown that layers of oxides formed on the outside surface featured the largest degree of surface development. For this surface parameters Ra, Rq and Rmax were 297 nm, 365 nm and 2097 nm, respectively. In the case of the inside surface Ra and Rq parameters were lower by a few dozen units, while Rmax lower by as much as 600 units.

a)

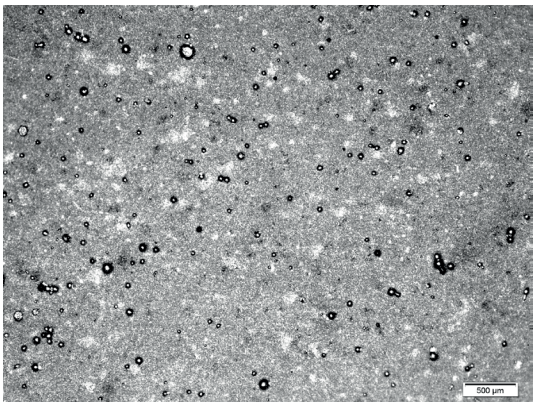

b)

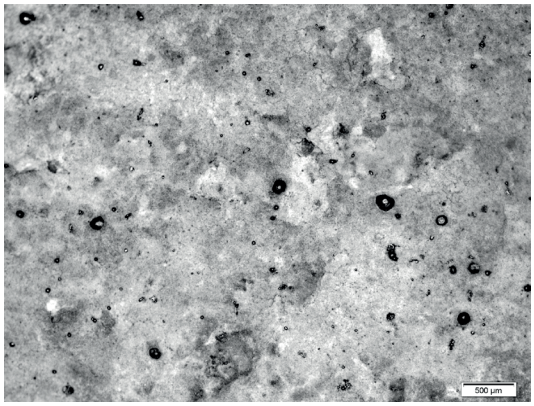

Fig. 2. Oxides formed on 13CrMo4-5 steel operated at 470°C during 190,000 hours: (a) inner surface, LM, (c) outer surface, LM

a)

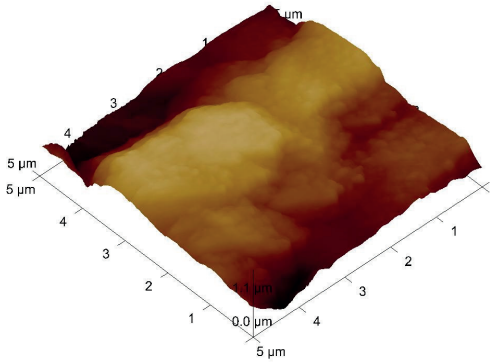

a)

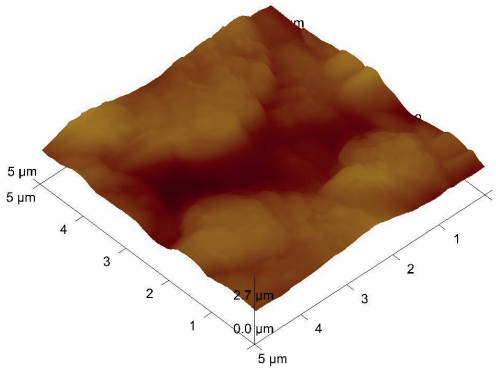

Fig. 3. Surface topography (3D) of the oxides layer, formed on the 13CrMo4-5 (AFM) steel: (a) inner surface, (b) outer surface

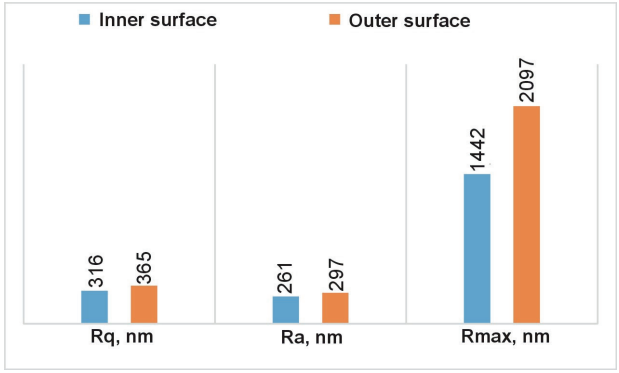

Fig. 4. Stereometric parameters, Rq – root meat square, Ra – roughness average, Rmax – maximum roughness depth

Observations of transversal microsections have shown (Fig. 5, 6) that both on the outside and on the inside there is corrosion along grain boundaries. On the inside the corrosion is small, while on the outside it is significant, which is presented in Fig. 7. In addition, the steel structure at the outside surface features a substantial decarburisation (Fig. 8). In this structure, apart from the ferrite, there are numerous carbide precipitates and creep micropores. The maximum thickness of the oxide layer on the inside was ~57 µm, while on the outside the oxides layer with deposits was 160 µm thick. Observations of the inside have shown that the formed layer is compact, featuring a small porosity. Only locally microfissures exist in this layer, situated mainly parallel to the surface. Instead, in the case of the outside layer its thickness observed was diversified. The layer of deposits formed directly on the side of flue gas inflow features spalling (Fig. 6b), which was confirmed by AFM studies. In the widest place the layer of deposits was 74 µm thick. Under this layer there is a layer of hematite (Fe_2O_3), maximum 70.35 µm thick, under which there is magnetite (Fe_3O_4), 50.39 µm thick.

a)

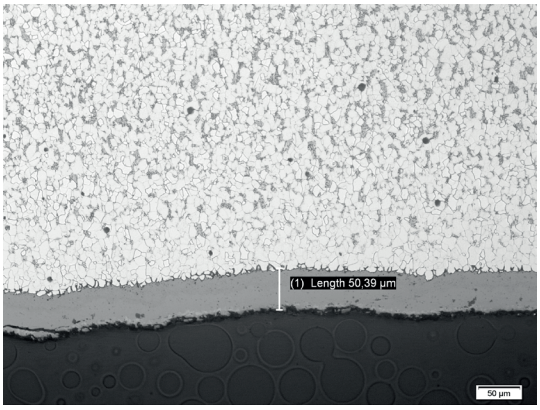

b)

c)

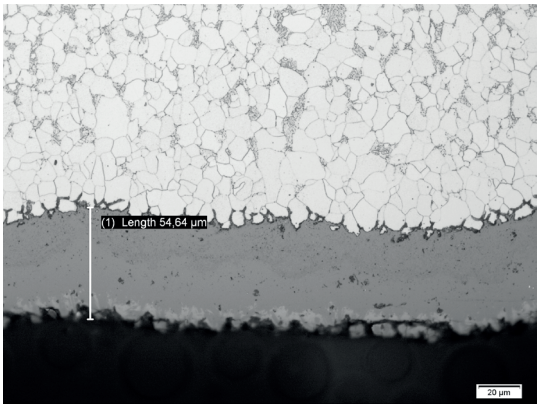

d)

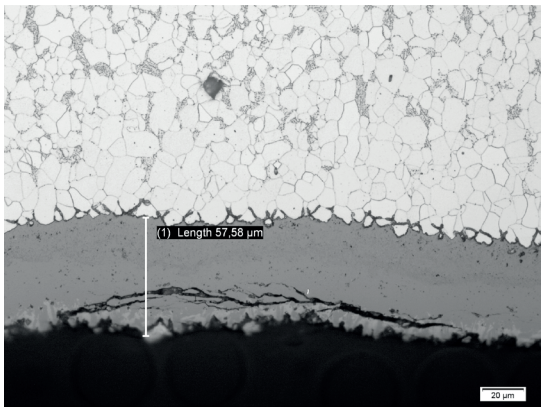

Fig. 5. The thickness of oxides layer formed on the steel examined, inner surface, LM: (a-d) varied thickness

a)

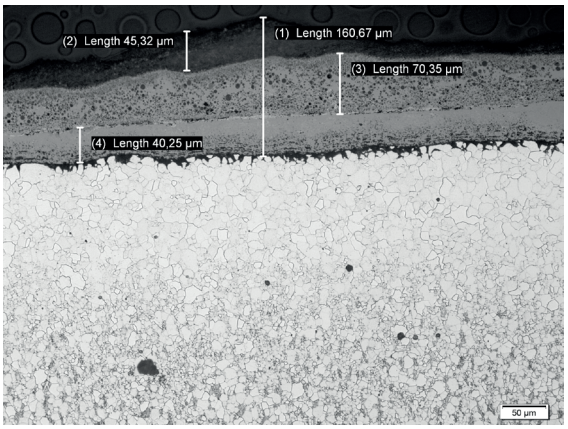

b)

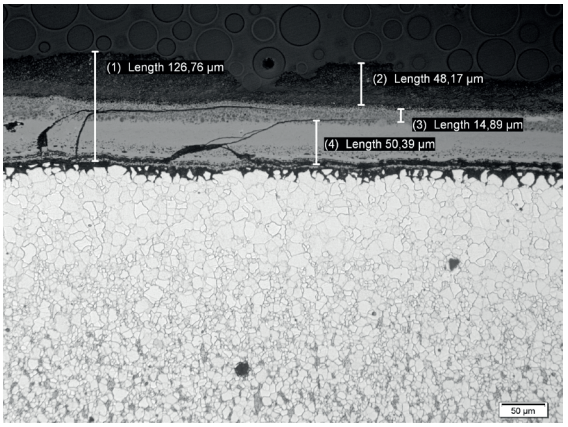

c)

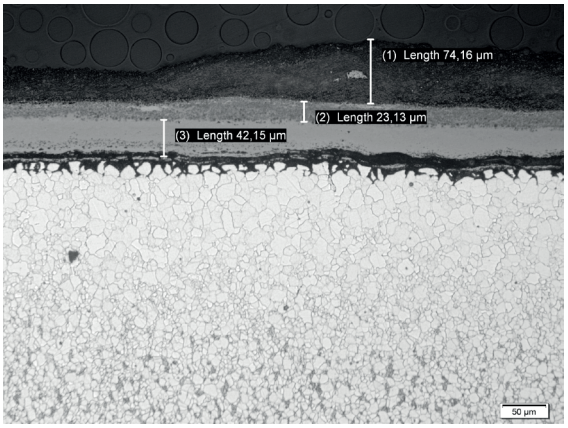

Fig. 6. The thickness of oxides layer formed on the steel examined, outer surface, LM: (a-c) varied thickness

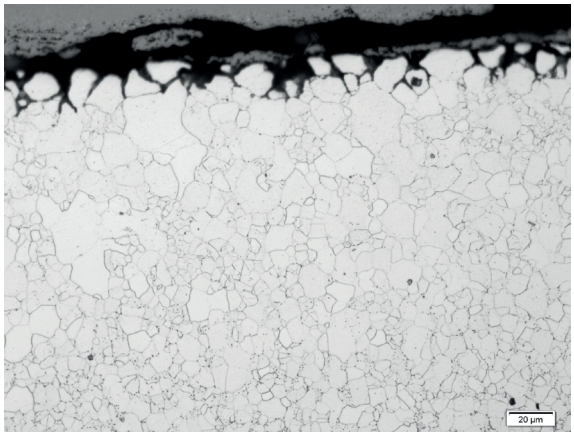

Fig. 7. Corrosion on the grain boundaries at the outside surface

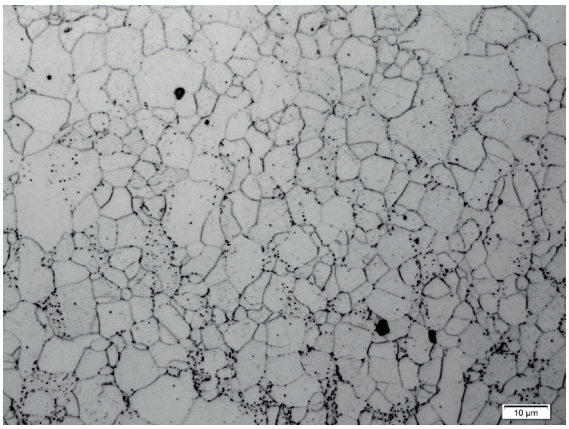

Fig. 8. Decarburisation of steel occurring at the outside surface

Performed EDS analysis of chemical composition (Fig. 9) combined with X-ray phase analysis (Fig. 10) has shown that oxides occur on the inside surface of tube. Based on DHN PDS and PDF4+2009 crystallographic database it has been found that the forming oxides are: Fe_2O_3 and Fe_3O_4 in accordance with the catalogue card numbers: 01-079-0007, 01-089-0951, respectively. In the case of the outside surface of tube apart from the aforementioned compounds also As, Ca, C, Al, Si, Na, Zn, S and K based compounds exist, such as: As_2O_3 (15-0778), $CaCO_3$ (05-0433), $KAlSi_2O_6$ (17-0047), CaS (08-0464), Na_6ZnO_4 (28-1193), ZnO_2 (13-0311) and ZnO (21-1486).

a)

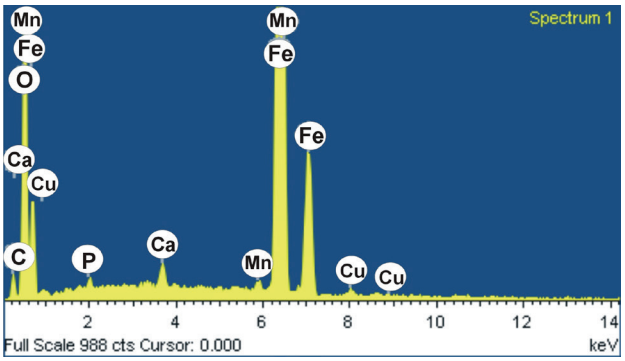

b)

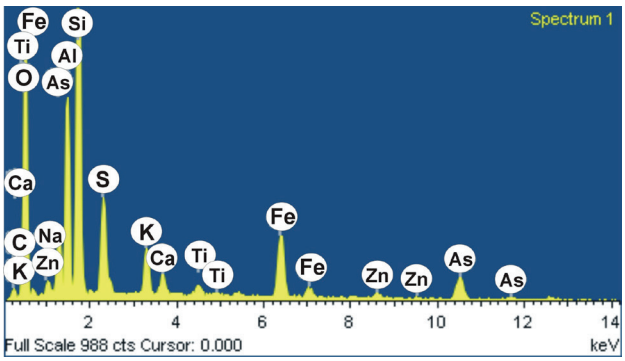

Fig. 9. EDS point microanalysis: (a) inner surface, (b) outer surface

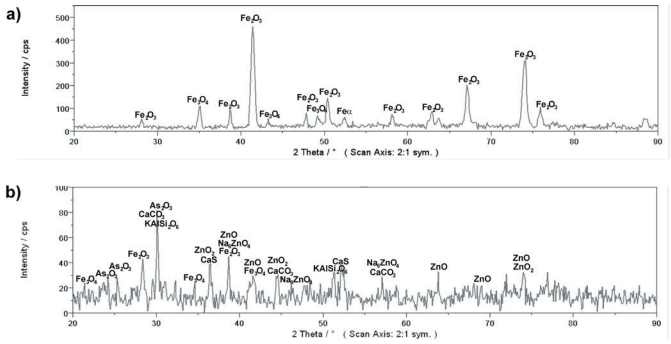

Fig. 10. Diffraction pattern of oxide layers obtained using the XRD technique: (a) inner surface, (b) outer surface

The scratch resistance characteristics have shown (Fig. 11) that for the inside a total delamination of the layer occurred at the load force of 100 N, while on the outside the magnetite layer was not entirely delaminated, which was confirmed by observations of scratch lines (Fig. 12). In the case of the inside at the maximum load of 200 N it is visible that the indenter has already pierced the native material (steel), while on the outside a spalling of deposits layer and of hematite is visible, instead, the magnetite layer remained intact.

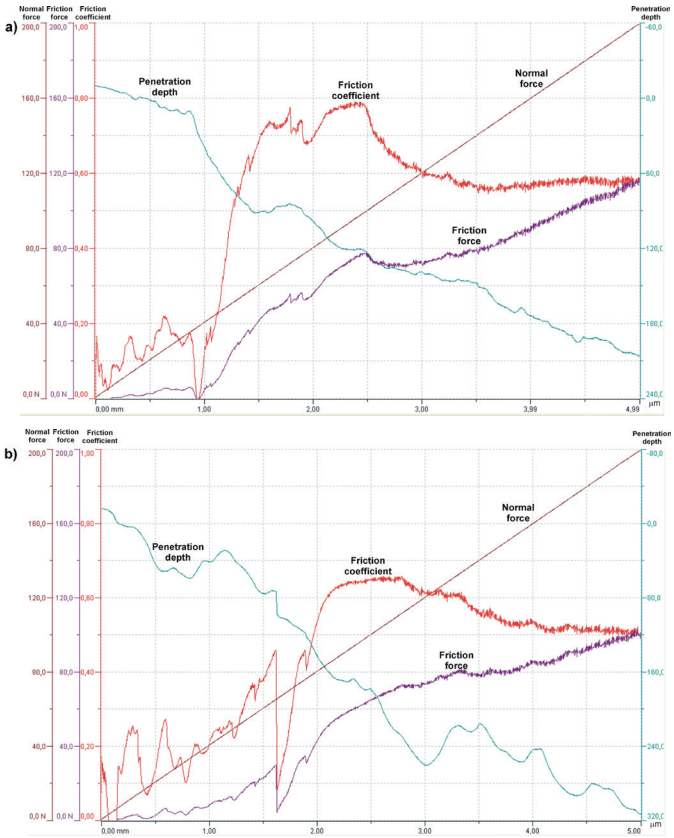

Fig. 11. Graph of data obtained from the scratch test for a preset force of 1÷200 N: (a) inner surface, (b) outer surface

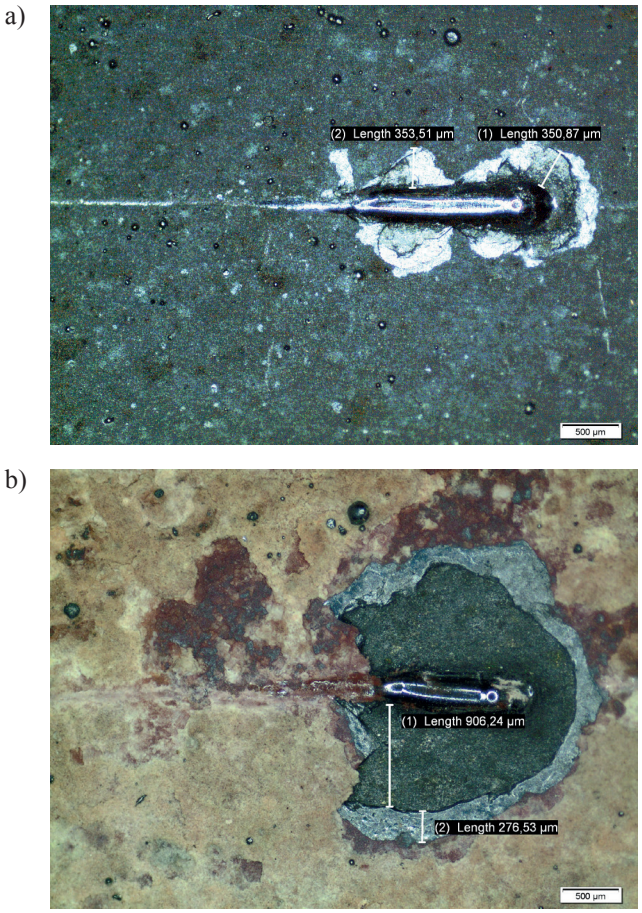

Fig. 12. Line of surface scratching: (a) inner surface, (b) outer surface

4. Summary

The obtained results of macro- and microscopic studies have shown that the layer of oxides/deposits formed on the studied steel on the flue gas inflow side is more degraded. A pretty thick (~74 µm) layer of deposits/oxides exists on this side, such as: As_2O_3, CaS, Na_6ZnO_4, ZnO_2, ZnO, $CaCO_3$ and $KAlSi_2O_6$. Under this layer hematite occurs, beneath which there is magnetite. A zonal structure of oxide layers was observed also on X10CrMoVNb9-1 [6-7] and 10CrMo9-10 [8] steels. In the oxides layer formed on the outside there are cases of spalling, which ale located mainly directly on the flue gas inflow side, while the porosity and microfissures exist in the oxides (Fe_2O_3 and Fe_3O_4) layer. Also on this side there is a significant corrosion along the grain boundaries. In the case of the inside surface hematite was the prevailing oxide phase, under which magnetite occurred. The other elements, such as Mn, Cu, Ca, C and P, occur in small amounts. Scratch resistance characteristics have shown that in the case of the outside surface the layer formed directly on the flue gas inflow side is brittle, also the hematite layer was damaged under the effect of load, while the layer of magnetite was not damaged even at the maximum load of 200 N. Studies performed on the inside surface have shown in turn that the layer delamination occurred at the load of 100 N.

REFERENCES

[1] A. Wocławski, A. Bernacik, J. Dobrzański, K. Śniegoń, K. Mandybur, P. Miliński, B. Doniec, Charakterystyka stali. Stale do pracy w temperaturach podwyższonych i obniżonych. Stale dla energetyki. Wydawnictwo „Śląsk", Katowice (1978).

[2] PN-EN 10028, Wyroby płaskie ze stali na urządzenia ciśnieniowe. Część 2: Stale niestopowe i stopowe o określonych własnościach w podwyższonych temperaturach.

[3] P. Gawron, F. Klepacki, Energetyka **6** (696) 293-303 (2012).

[4] P. Gawron, S. Danisz, Energetyka **12** (702) 843-853 (2012).

[5] P.J. Ennis, W.J. Quadakkers, International Journal of Pressure Vessels and Piping **84**, 75-81 (2007) .

[6] M. Gwoździk, Z. Nitkiewicz, Archives of Metallurgy and Materials **1** (58), 31-34 (2013).

[7] M. Gwoździk, Z. Nitkiewicz, Archives of Civil and Mechanical Engineering **14**, 335-341 (2014).

[8] M. Gwoździk, Z. Nitkiewicz, Solid State Phenomena **203-204**, 121-124 (2013).

[9] S. Frangini, A. Masci, S.J. McPhail, T. Soccio, F. Zaza, Materials Chemistry and Physics **144 (3)**, 491-497 (2014).

[10] J. Lehmusto, P. Yrjas, B.J. Skrifvars, M. Hupa, Fuel Processing Technology **104**, 253-264 (2012).

[11] J. Vaari, Solid State Ionics **270**, 10-17 (2015).

[12] X. Yu, Z. Jiang, J. Zhao, D. Wei, C. Zhou, Q. Huang, Corrosion Science **85**, 115-125 (2014).

[13] J. Bischoff, A.T. Motta, Journal of Nuclear Materials **424**, 261-276 (2012).

[14] X. Zhong, X. Wu, E.H. Han, Corrosion Science **90**, 511-521 (2015).

[15] J. Priss, H. Rojacz, I. Klevtsov, A. Dedov, H. Winkelmann, E. Badisch, Corrosion Science **82**, 36-44 (2014).

Received: 20 October 2014.